Aqueous Photochemistry of Secondary Organic Aerosol of α-Pinene and α-Humulene in the Presence of Hydrogen Peroxide or Inorganic Salts

Alexandra L. Klodt,[1] Dian E. Romonosky,[1] Peng Lin,[2] Julia Laskin,[2] Alexander Laskin,[2] Sergey A. Nizkorodov[1,*]

[1]Department of Chemistry, University of California, Irvine, CA 92697, USA

[2]Department of Chemistry, Purdue University, West Lafayette, IN 47907, USA

Keywords: aqueous photolysis, mass spectrometry, cloud/fog processing, molecular composition, ionic effects

ABSTRACT: The effect of common atmospheric solutes on aqueous-phase aging of secondary organic aerosol (SOA) was explored under irradiated and dark conditions. SOA particles were produced from dark ozonolysis of α-pinene or α-humulene in a photochemical smog chamber, collected on filters, and extracted in either pure water or in aqueous solutions containing 0.010 mM H_2O_2, 0.15 mM $NaNO_3$, or 0.15 mM NH_4NO_3. These aqueous samples were either irradiated for up to four hours to simulate photochemical aqueous aging by sunlight or kept in the dark for the same amount of time to simulate nighttime aqueous chemistry of SOA. The chemical composition of SOA was monitored over time using direct infusion electrospray ionization high-resolution mass spectrometry. The presence of salts accelerated the loss of high-molecular weight compounds, both under irradiated and dark conditions, making the dissolved SOA compounds smaller and more volatile. These effects of atmospheric salts have important implications for understanding SOA evolution in cloud and fog water.

INTRODUCTION

Secondary organic aerosol (SOA) has a significant impact on human health and climate, and it is therefore important to understand how SOA particles are produced from volatile organic compounds (VOCs) and age during particle transport through the atmosphere.[1] Monoterpenes ($C_{10}H_{16}$) are the major atmospheric SOA precursors with atmospheric concentrations of hundreds to thousands of ppt,[2] and SOA formation from various monoterpenes, particularly α-pinene,[3] has been studied extensively.[4–7] There have also been studies on SOA formation from sesquiterpenes ($C_{15}H_{24}$) such as α-humulene,[8] which are less abundant in the atmosphere (measured to be tens of ppt)[2] but have greater SOA yield due to their higher molecular weights.[9] The lifetimes of monoterpenes and sesquiterpenes for reaction with atmospheric oxidants are generally minutes to hours,[6] and so they are quickly oxidized to compounds that can be soluble in cloud and fog water.

Chemistry occurring in fog and cloud droplets is known to be a significant factor in both the formation and aging of SOA.[10] For example, 5 to 60% of SOA globally is estimated to result from in-cloud processing,[11] and reactions occurring in the atmospheric aqueous phase have been proposed to explain the discrepancies in SOA oxidation level observed between laboratory and field studies.[12,13] Atmospheric fog and cloud waters often contain approximately 200 μg mL^{-1} of dissolved organics,[14,15] as well as aqueous oxidants, such as H_2O_2 with normal concentrations of around 10^{-6} M, and inorganic salts. These inorganic salts, usually ammonium nitrate or ammonium sulfate, result in ionic strengths ranging from 10^{-4} to 10^{-2} M in fog water and 10^{-5} to 10^{-2} M in cloud water,[10] and can potentially affect the aging mechanisms of aqueous SOA. For instance, NO_3^- can serve as a photochemical source of OH radicals,[16] NH_4^+ can react with carbonyls and act as a catalyst for various reactions,[17,18] and changing ionic strength can affect acid-base or other aqueous equilibria as salts can act as buffers in aqueous solutions. There have been only a few studies probing the effects of common inorganic salts on aqueous-phase photochemical aging of SOA.[19,20] Even small concentrations of added solutes can have a significant effect on photochemistry, for example, Huang et al. (2018) found that

photodegradation rates of syringaldehyde and acetosyringone in micromolar nitrate solutions were faster than rates in sulfate solutions.[21]

Mechanisms of aqueous SOA aging can be photolytic or non-photolytic, and the photolytic processes can be further categorized as direct or indirect. The direct aqueous-phase photolysis of SOA extracts in pure water and in water/methanol mixtures has been examined in several studies.[22–25] The irradiation of SOA solutions resulted in a reduction in the average molecular size of SOA compounds driven by Norrish splitting of carbonyls and photolysis of peroxides.[26,27] Indirect photolysis occurs in parallel when reactions with sunlight produce reactive species, such as OH radicals, singlet oxygen, or triplet-excited states, and then these species react with SOA components. In contrast to the direct photochemical processes, the indirect processes normally result in more functionalized and less volatile products.[28] Non-photolytic aging pathways include hydrolysis[29,30], functional group exchange with inorganic ions, and reactions with other oxidizing solutes – H_2O_2 in this work. In the hydrolysis of esters, the starting compounds are fragmented to smaller molecules with carboxyl and alcohol groups, resulting in smaller products with higher vapor pressures. Certain reactions with inorganic salts can decrease vapor pressure as salts are formed between carboxylic acids and inorganic cations.[31,32] Finally, the presence of H_2O_2 can have a myriad of consequences. Neglecting its host of influences on photochemical reactions, H_2O_2 is an important aqueous-phase oxidant,[10] its reactions with carbonyls and alcohols can produce peroxides, [33]it is well known to be an important part of sulfate formation from SO_2,[34] and can be a source of radicals in the dark through Fenton-type reactions. [35]

Previous studies from our group have explored the aging of SOA from various terpenes, including those studied here, in pure water.[24,36] The present work is intended to implement a more atmospherically relevant approach by adding solutes as would be present in atmospheric cloud and fog waters. Thus, the goals of this study are (1) to ascertain whether the photolysis and dark aging of aqueous SOA in the presence of common atmospheric solutes proceeds via a different mechanism compared to in the absence of these solutes and (2) to compare photolytic and dark aging of SOA in the presence of ionizable versus non-ionizable solutes. To

accomplish these goals, aging of SOA produced from ozonolysis of a common monoterpene, α-pinene (APIN), and a common sesquiterpene, α-humulene (HUM), was studied using high-resolution mass-spectrometry after the SOA was aged in various conditions. These conditions included the presence or absence of both sunlight and solutes such as hydrogen peroxide (as a non-ionizable solute), sodium nitrate (an ionizable solute), and ammonium nitrate (an ionizable solute that also provides ammonium as a reactant).

METHODS

Secondary Organic Aerosol Generation. APIN and HUM SOA were prepared through dark reaction with O_3 as described in previous papers.[24,36,37] APIN and HUM were purchased from Sigma-Aldrich at the highest available purity, and no further purification was performed. Approximately 600 ppb O_3 and 500 ppb of precursor were injected into a 5 m^3 chamber, and ozonolysis was allowed to proceed under dry conditions at 21 to 25 ^oC without seed particles. These relatively high concentrations were necessary to obtain enough material for subsequent photochemical and mass spectrometric experiments. Particle sizes were monitored using a TSI model 3936 scanning mobility particle sizer (SMPS) and ozone concentrations were monitored using a Thermo Scientific model 49i ozone analyzer. An Aerosol Mass Spectrometer (AMS) was not used during the generation of the SOA used for aging, but AMS data was later collected during the generation of HUM SOA produced under the same conditions for additional solubility experiments. Aerosol particles were subsequently collected onto poly(tetrafluoroethylene) (PTFE) filters (Millipore 0.2 μm pore size) after passing through an activated carbon denuder with a flow rate of about 10 SLM (standard liters per minute). Two filter samples were collected over 2 to 3 h during each chamber experiment. A breakdown of SOA production details is provided in Table 1. After collection, the samples were vacuum sealed and frozen at -20 ^oC pending aqueous photolysis experiments.

Table 1. Conditions used for SOA preparation. SOA concentration represents maximum during collection of two sequentially collected filters, and so the concentrations are different.

Filter #	VOC	Initial VOC	Initial O_3 (ppb)	Reaction Time (h)	Peak SOA concentration	Collection Time	SOA collected

		(ppb)			(mg/m^3)	(hr)	(mg)
1	APIN	500	600	0.8	1.5	1.5	1.8
2	APIN	500	600	0.8	0.96	1.5	1.8
3	HUM	500	600	2	1.7	1	2.1
4	HUM	500	600	2	1.4	1	2.0

Table 2. Summary of aqueous samples prepared from SOA filters. Aqueous SOA concentration assumes full dissolution for APIN SOA and 40% dissolution for HUM SOA (see main text for discussion).

T

VOC	Filter #	Aqueous oxidant/salt	Aqueous SOA concentration (µg/mL)	Aqueous oxidant/salt concentration (mM)
APIN	1	N/A	184	N/A
APIN	1	H_2O_2	177	0.010
APIN	2	$NaNO_3$	180	0.15
APIN	2	NH_4NO_3	180	0.15
HUM	3	N/A	84	N/A
HUM	3	H_2O_2	80	0.010
HUM	4	$NaNO_3$	78	0.15
HUM	4	NH_4NO_3	78	0.15

Secondary Organic Aerosol Aging Experiments. Samples were thawed, and each filter was extracted with 10 mL of HPLC grade water. After sonicating for about 10 min, the water and SOA solutions were split into 4 aliquots of 2.5 mL and 100 µL of concentrated aqueous oxidant or salt solution was added with final concentrations as shown in Table 2. No precipitation of SOA was observed after the addition of these small concentrations of salts, so we do not believe the added salts had a significant impact on the SOA solubility. Under these conditions, we expect all APIN SOA to dissolve based on previous water solubility studies of similarly prepared monoterpene SOA.[38] HUM SOA water extraction efficiency has not been tested before, and we estimated it by extracting the filter first in water and then in methanol and comparing absorption spectra of the extracts. Based on this comparison, we expect that water extraction dissolved about 40% of the HUM SOA material (Figure S2). The concentrations shown in Table 2 have been corrected for this incomplete extraction. Because some HUM SOA remains undissolved, the results of these experiments only apply to the water-soluble fraction.

Photolysis occurred similarly to our previous paper;[24] control samples were simultaneously aged under dark conditions. Briefly, a Xenon UV lamp (Newport model 66905) was used with a U-330 bandpass filter (Edmund optics #46-438) to decrease levels of hard UV, visible, and IR radiation. The majority of the radiation fell between 280 and 400 nm. Using the "Quick TUV"[39] calculator, and we determined the lamp's flux to be comparable to that under ambient conditions (a full analysis is provided in Figure S1 and Table S1). Therefore, the photolysis time under the UV lamp can be viewed as equivalent to photolysis in sunlight during summertime in Los Angeles. OH steady state concentrations produced by photolysis of added H_2O_2 and NO_3^- were determined to be too low to have a significant effect on the aging of SOA, as they were estimated to be about 10^{-18} M in all conditions where OH was produced (see Table S2 and accompanying discussion in the Supporting Information). The photolysis and control (i.e., without photolysis) experiments were done for four hours. Samples of the solutions were taken once every hour for off-line analysis using direct infusion electrospray ionization high-resolution mass spectrometry (ESI-HRMS).

Mass Spectrometry Analysis. Approximately 200 µL of sample was mixed in a 1:1 ratio with acetonitrile to achieve stable electrospray ionization and then injected into the mass spectrometer using a direct infusion mode. An LTQ-Orbitrap mass spectrometer (Thermo Scientific ™) equipped with a modified ESI source was used to analyze the samples.[22,23,36,37,40–43] Mass spectra of the solvent (water and acetonitrile) were also collected so that background spectra could be subtracted from the sample spectra. A representative solvent spectrum is shown in Figure S13. All spectra were collected in the positive ion mode, and the resolving power of the instrument was ~10^5 at *m/z* 400.

The analysis of the mass spectra was carried out similarly to our previous work.[36,44] Peak positions and intensities were first determined using Decon2LS program (https://omics.pnl.gov/software/decontools-decon2ls), and the resultant peak lists were clustered together according to experimental batch, such that 0, 1, 2, 3, and 4 h with photolysis was a group for each experimental condition and 0, 1, 2, 3, and 4 h without photolysis was another group. The clustered peaks were then assigned assuming a 0.001 *m/z* accuracy with

formulas of $C_cH_hO_xN_nNa_s$. The number of nitrogen atoms per molecule was allowed to be between 0 and 3. The number of sodium atoms was also allowed to be between 0 and 3. The monosodium adduct was the most common ion peak in nearly all cases, but some adducts corresponding to two sodium minus one hydrogen and even a few adducts corresponding to three sodium minus two hydrogens were observed. Sodium adducts are commonly observed in direct infusion electrospray ionization, and they can be formed during ionization within the instrument.[45,46] But since it is unusual to have more than one sodium ion in the ions, we made sure that these peaks could not be explained by isotopes or possible impurities. We assume that the intentional addition of $NaNO_3$ in some of our experiments enhanced the sodium adduct formation.

Nitrogen was allowed in the assignments of the pure water and H_2O_2-containing samples, but subsequent nitrogen-containing assignments for these trials were negligible. Elemental ratios for assigning were constrained to $0 < O/C < 1.3$ and $0.7 < H/C < 2.0$ to ensure the assignment of physically reasonable formulas.[47] ^{13}C isotopes and obvious impurities with anomalous mass defects were not considered for the remainder of the analysis. Assigned peaks were then used to check the internal calibration of the *m/z* axis. Peaks that were unassigned and peaks with questionable suggested formulas were re-assigned manually using a molecular formula calculator (http://magnet.fsu.edu/~midas/). In the case of the samples containing ammonium nitrate, it was possible for peaks to have been ionized by ammonium. Therefore, in these trials, peaks containing nitrogen were examined individually to determine whether this was the case. Since the majority of the peaks were ionized by sodium, only peaks with a large analogous sodium ion adduct peak and an unusually high H/C ratio (from the 4 extra H-atoms in NH_4^+) were assumed to be ammonium ion adducts. Lastly, the formulas of the assigned ions were converted to the neutral formulas by removing Na^+, H^+, or NH_4^+, depending on the ionization mechanism. Hereafter, all the identified compounds are presented and discussed as neutral species with their corresponding masses.

RESULTS AND DISCUSSION

Effect of Aging on APIN SOA Mass Spectra

The presence of aqueous oxidants and salts in SOA extracts under irradiated and dark conditions can be expected to foster different chemical pathways for SOA aging. In experiments where only SOA is dissolved in pure water, photolysis and hydrolysis of SOA compounds can occur in parallel:

1. $SOA + hv, H_2O \rightarrow products$

In the presence of hydrogen peroxide, there can be additional reactions between SOA and H_2O_2 or reactions driven by oxidation of SOA compounds with OH:

2. $H_2O_2 + SOA \rightarrow products$
   $H_2O_2 + hv \rightarrow 2\ OH$
   $SOA + OH \rightarrow products$

Nitrate photolysis produces OH radicals and nitrating agents such as NO_2 which may react with SOA to form nitrogen containing organic compounds (NOC),[16] so nitrate ions can influence the products of photolytic SOA aging.

3. ${NO_3}^- + H_2O + hv \rightarrow {NO_2}^- NO_2 + OH + OH^-$
   $SOA + NO_2 \rightarrow NOC$
   $SOA + OH \rightarrow products$

For solutions where ammonium salts are present, competing reactions between carbonyls and ammonia can occur, generating reduced NOC,[48,49] as well as various reactions catalyzed by ammonia:[17,18]

4. $SOA \xrightarrow{{NH_4}^+} products$

Finally, the presence of salts changes the ionic strength of solutions, which can indirectly affect reactions such as hydrolysis. The OH concentrations present in our solutions was very low, so OH and other radical reactions will be neglected during our analysis. However, we will be

looking for evidence of the other processes in the mass spectra, as described below.

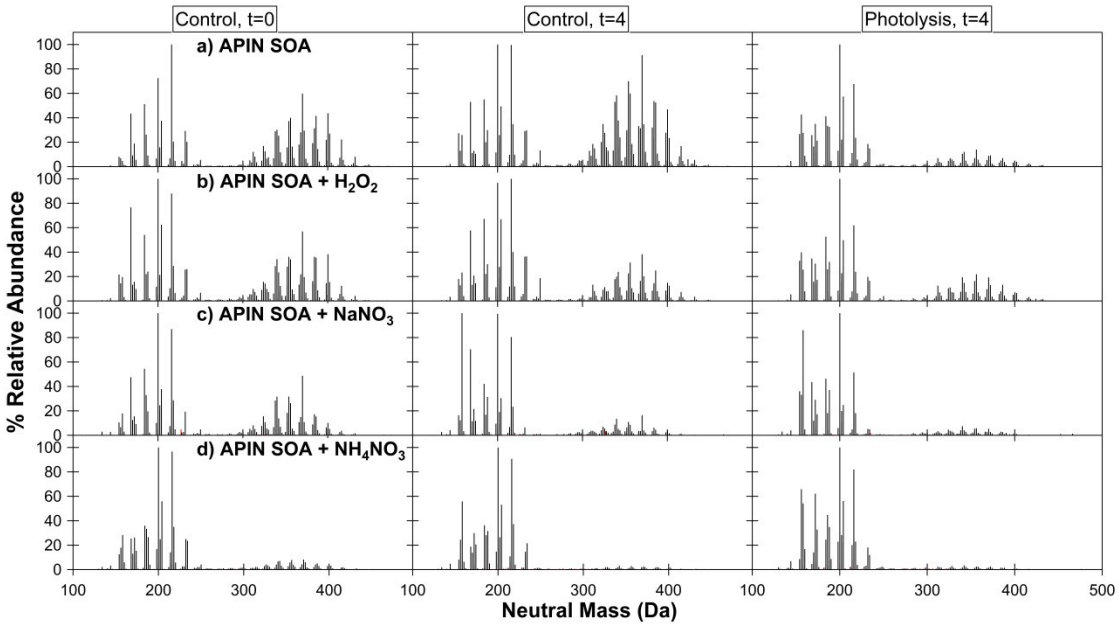

Figure 1. HRMS spectra are shown for APIN SOA aged in nanopure water (a), and aqueous solutions containing 0.01 mM H_2O_2 (b), 0.15 mM $NaNO_3$ (c), and 0.15 mM NH_4NO_3 (d) taken for 0 h, the dark control at 4 h, and the photolysis sample at 4 h. Peaks are normalized to the highest peak in each spectrum. No significant peaks were observed above 500 Da, so this region is not shown. NOC peaks are plotted in red, but difficult to see in the figure without magnification. These peaks may more easily be seen in Figure S11.

Figure 1(a) shows the mass spectra of the original (unreacted) APIN SOA solution in water and after 4 h in both the photolysis and dark experiments. Mass spectra obtained for the full time series are shown in Figures S3-S10. Peaks are normalized to the highest peak in each spectrum. The mass spectra are similar to previously reported APIN SOA ozonolysis spectra,[24,36,50–53] for example, the monomer (<300 Da, a single oxygenated APIN unit) and dimer regions (300 – 500 Da, two covalently-bound oxygenated APIN units) can be clearly discerned. $C_{10}H_{16}O_5$ (MW 216), $C_{10}H_{16}O_4$ (10-hydroxypinonic acid), and $C_{10}H_{16}O_3$ (pinonic acid) appear as the most abundant monomers. $C_{19}H_{30}O_7$ (MW 370) and $C_{19}H_{30}O_8$ (MW 386), which were identified as ester compounds when observed in boreal forest field studies in Hyytiälä, Finland,[54] are the major

detected dimers.[55] A more detailed list of peaks of interest can be found in Table 3. Another feature of Figure 1(a) is a reduction in the relative abundance of dimers as compared to monomers with photolysis, but not in the dark condition, as observed previously in experiments in pure water.[24] This relationship may more easily be seen in Figure 2, which shows all dimer/monomer ratios for the systems discussed.

Table 3. Some of the major compounds detected in the APIN SOA by mass spectrometry. Photolyzable groups are shown in red, and hydrolyzable groups are shown in blue. Some of the compounds have multiple suggested structures which have been included. Special emphasis is placed on dimers, as they are of particular interest in this paper.

Observed Molecular Weight (Da)	Relative Abundance (%)	Compound Formulas and Suggested Structures	Structure Reference
184	51	Pinonic Acid – $C_{10}H_{16}O_3$ – Monomer 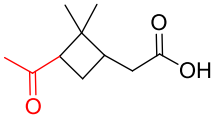	[55]
200	72	10-hydroxypinonic acid – $C_{10}H_{16}O_4$ – Monomer 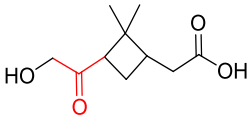	[55]
216	100	$C_{10}H_{16}O_5$ – Monomer 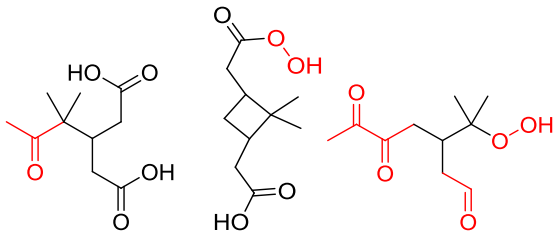	[56–58]
338	29	$C_{19}H_{30}O_5$ – Dimer 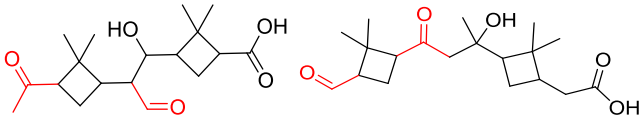	[59]

340	30	$C_{18}H_{28}O_6$ – Dimer 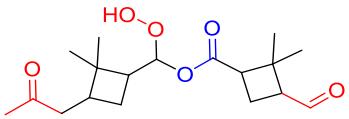	59
356	40	$C_{18}H_{28}O_7$ – Dimer 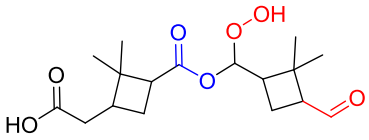	54
358	16	$C_{17}H_{26}O_8$ – Dimer 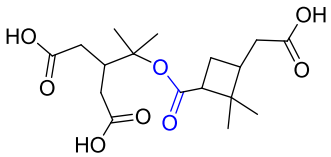	60
368	28	$C_{19}H_{28}O_7$ – Dimer 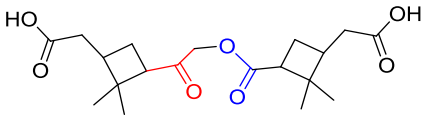	60
370	60	$C_{19}H_{30}O_7$ – Dimer 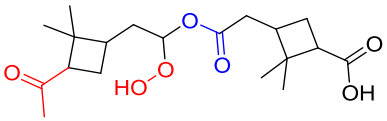	54

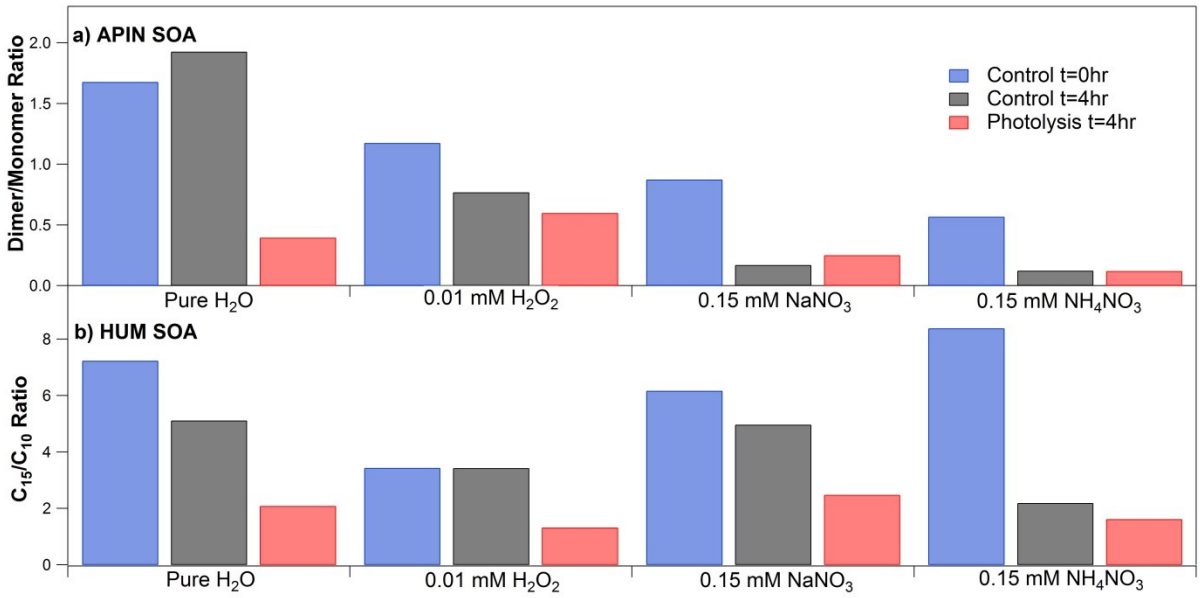

Figure 2. Dimer/monomer ratios and C_{15}/C_{10} ratios for APIN SOA (a) and HUM SOA (b), respectively, are shown for 0 h, the dark control at 4 h, and photolysis at 4 h. Data are grouped by aqueous aging conditions. Ratios are calculated by dividing the total dimer by the total monomer peak abundance or the total C_{15} by the total C_{10} peak abundance. These ratios are analogous in the sense that monomer and C_{10} peaks both represent lower molecular weight aging products in the performed experiments. Further explanation of C_{10} and C_{15} peaks is provided in the section discussing the effect of aging on HUM SOA mass spectra.

Figure 1(b) shows the HRMS spectra acquired from the APIN SOA + H_2O_2 experiment. The spectra are qualitatively similar to those of APIN SOA in pure water (Figure 1(a)). Again, there is a greater decrease in the dimer region of the spectra in the presence of H_2O_2 than in the dark, as shown in Figure 2. However, the relative abundance of dimers is actually larger in Figure 1b (after irradiation of SOA with H_2O_2) than in Figure 1a with photolysis (after irradiation of SOA in pure water).We theorize that this may be a result of the formation of peroxyhemiacetals from reactions of H_2O_2 and carbonyls present in the SOA.[33] This would decrease the rate of decay as the lifetimes of carbonyls [61] have been estimated to be shorter than the lifetimes of peroxides[62] at wavelengths above 300 nm, as are present in this study.

The most interesting feature of Figure 1 is the effect of nitrate salts on APIN SOA aging in the dark. Under these conditions, a large reduction in the relative abundance of dimers was observed. This is a significant departure from the minor effect of dark reactions in the pure water and H_2O_2 conditions (also illustrated in Figure 2). The reduction in dimers in both the photolysis and control conditions was much more significant in the presence of nitrates than in the other conditions. One possible explanation for the observed dark chemistry is that nucleophilic compounds, particularly oxyanions, have been shown to catalyze hydrolysis of esters,[63] which are prevalent among dimers in APIN SOA. We compared the final mass spectra of the photolysis and dark reactions with nitrate in hope of finding unique peaks attributable to hydrolysis, but no systematic difference between peaks in irradiated and non-irradiated solutions was observed. The hydrolysis reaction converts dimers to monomers, which are also present in solution to begin with, making it hard to identify a signature of hydrolysis chemistry.

An additional aspect of the APIN + NH_4NO_3 experiment is that the dimer region in the t=0 panel (Figure 1(d)) is already smaller than in the other experiments, even as compared to the analogous APIN + $NaNO_3$ experiment (Figure 1(c)). This implies that there was a significant reduction in dimers already in the short time between the ammonium nitrate being added and the sample being analyzed by HRMS (about 10 minutes). Some of the reduction in the dimer peak abundances may also be due to ionization suppression effects known to be caused by the presence of salts in electrospray,[64] but the further reduction in the dimer peaks following hydrolysis and photolysis suggests that the ionization suppression effects cannot be solely responsible for our observations.

Effect of Aging on HUM SOA Mass Spectra

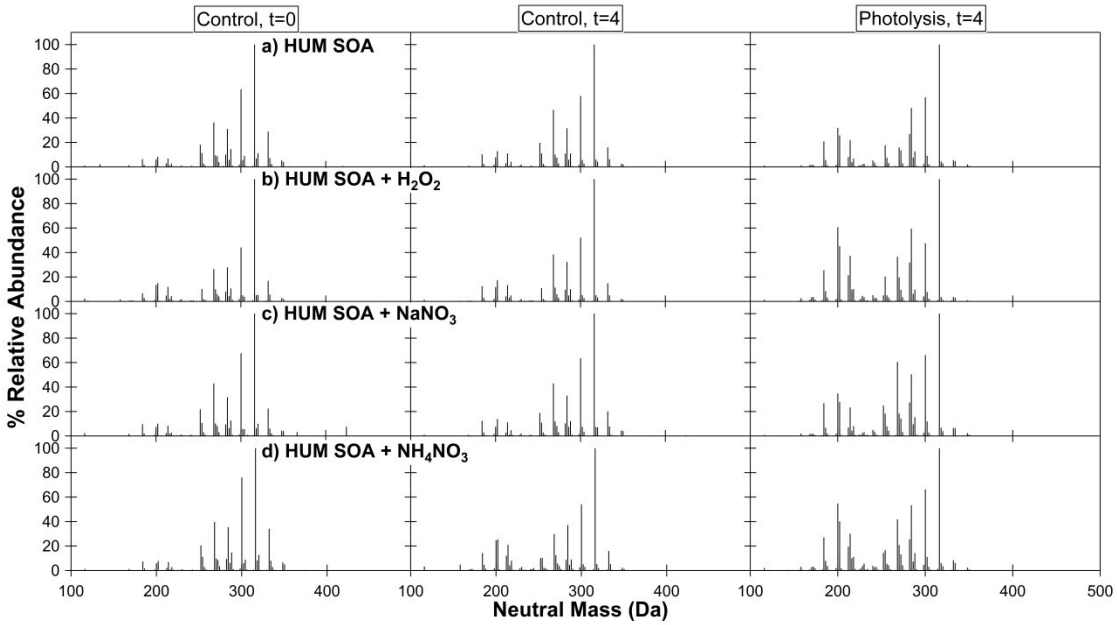

Figure 3. HRMS of HUM SOA aged in nanopure water (a), and aqueous solutions containing 0.01 mM H_2O_2 (b), 0.15 mM $NaNO_3$ (c), and 0.15 mM NH_4NO_3 (d) taken for 0 h, the dark control at 4 h, and the photolysis sample at 4 h. Peaks are normalized to the highest peak in each spectrum. NOC peaks are plotted in red, although these peaks all have % Relative Abundances of less than 1 and cannot be readily seen. Data is replotted in Figure S12 to show these peaks.

Mass spectra of HUM SOA in pure water are shown in Figure 3(a). The majority of the peaks are clustered around the C_{15} region that makes up the HUM carbon backbone. The largest peaks in the spectra are shown in Table 4, and have formulas $C_{15}H_{24}O_o$ where *o* ranges from 4 to 8, with the most abundant compound in each spectrum being $C_{15}H_{24}O_7$. For the HUM SOA, the first generation ozonolysis products of HUM have vapor pressures sufficiently low to form particles, and dimers are low in abundance.[65] There are a few compounds in the C_{10} region (clustered around a mass of 200 Da) which have been reported in previous studies,[8,24] and seem to be common products of the fragmentation of HUM. The abundances of C_{10} peaks increase relative to those of C_{15} peaks with photolysis, but there is no significant change in the overall C_{15}/C_{10} peak ratio under dark conditions in water.

Table 4. The major compounds detected in the HUM SOA before aging. The only previously identified HUM SOA compound structure is included.[8]

Observed Molecular Weight (Da)	Relative Abundance (%)	Compound Formula
268	36	$C_{15}H_{24}O_4$ 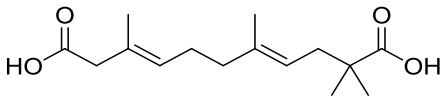
284	31	$C_{15}H_{24}O_5$
300	63	$C_{15}H_{24}O_6$
316	100	$C_{15}H_{24}O_7$
332	29	$C_{15}H_{24}O_8$

The effects of salts and H_2O_2 were less prominent for HUM SOA than for APIN SOA. Figure 3(b) and Figure 2 show that HUM SOA experiences carbon chain shortening from photolysis with H_2O_2, as higher relative abundances of C_{10} compounds were observed after four hours of photolysis with H_2O_2. This is qualitatively similar to the results for APIN SOA. Comparing the pure water experiment (Figure 3a) with the HUM SOA + $NaNO_3$ experiment (Figure 3b), the presence of NO_3^- had little effect on the aging of the HUM SOA. This suggests that esters, which are present in APIN SOA and may be hydrolyzed with nitrate, are not as abundant in HUM SOA. There is a more dramatic decrease in the C_{15}/C_{10} ratio in the HUM SOA + NH_4NO_3 condition (Figure 2) but the final mass spectrum after four hours is not too different from the mass spectra observed under other conditions.

Effect of Aging on Elemental Ratios

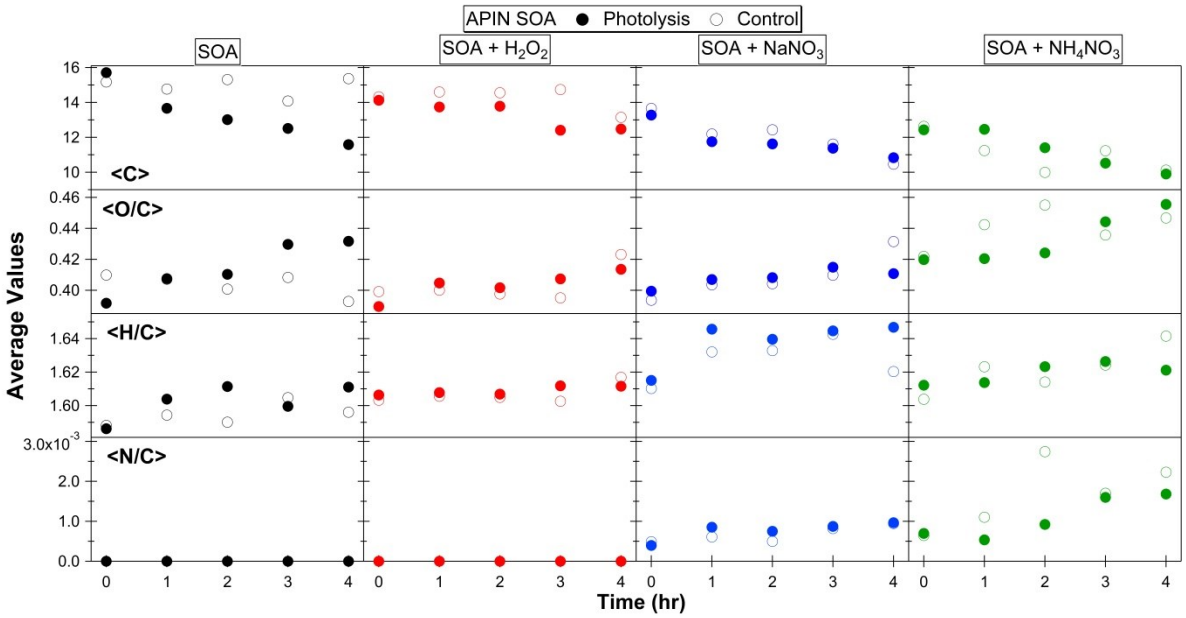

Figure 4. Average values for the number of carbon atoms, O/C ratios, H/C ratios, and N/C ratios are shown at each hour of the four-hour aging time of APIN SOA in nanopure water, 0.01 mM H_2O_2, 0.15 mM $NaNO_3$, and 0.15 mM NH_4NO_3. Open circles denote the dark control condition, and closed circles denote the photolysis condition.

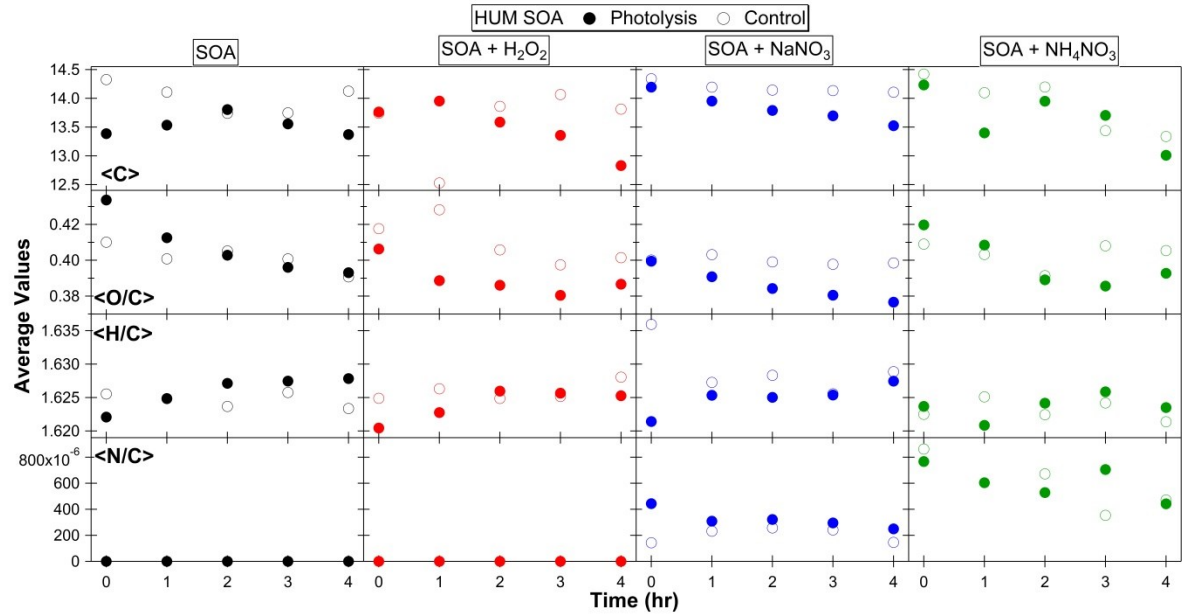

Figure 5. Average values for the number of carbon atoms, O/C ratios, H/C ratios, and N/C ratios are shown at each hour of the four-hour aging time of HUM SOA in nanopure water, 0.01 mM H_2O_2, 0.15 mM $NaNO_3$, and 0.15 mM NH_4NO_3. Open circles denote the dark control condition, and closed circles denote the photolysis condition.

O/C, H/C, and N/C values are reported in Figures 4 (APIN SOA) and 5 (HUM SOA) as a function of reaction time. Average carbon number is also reported in these figures to illustrate the average molecular size at each time point. These average values were calculated from the neutral molecular formulas using the equation shown below, where I_i are the peak abundances:

$$\langle x \rangle = \frac{\Sigma I_i x_i}{\Sigma I_i} \text{ (x = \#C, H/C, O/C, N/C)}$$

As elemental ratios are of great interest to the AMS community, we compared the O/C and H/C ratios calculated from ESI-MS to those measured by the AMS when making the HUM SOA. Generally, O/C ratios calculated from ESI-MS are expected to be similar to those calculated by the AMS and have comparable accuracy.[40] In this study we found our O/C and H/C values to be similar between the two instruments, though not exactly the same. The O/C ratio was about 0.40 when determined by ESI-MS and 0.37 when determined by AMS. The H/C ratios were 1.63 and 1.80 by ESI-MS and AMS, respectively. Considering that ESI-MS and AMS probe a different subset of molecules in SOA, this represents a good level of agreement.

Figures 4 and 5 show that APIN SOA and HUM SOA contain molecules of similar average carbon number (~C_{15}). This is due to the comparable abundance of monomers (C_{10}) and dimers (C_{20}) in the APIN SOA mass spectra and the predominance of monomers (C_{15}) in the HUM SOA mass spectra. The average carbon number decreased under all irradiated conditions indicating that APIN SOA dimers are degraded and HUM SOA C_{15} compounds are converted to C_{10} compounds with photolysis. Most of the samples aged in the dark did not exhibit a significant decrease in carbon number with reaction time. Two exceptions are the APIN SOA control experiments containing nitrate salts and the HUM SOA experiment containing ammonium. In these experiments, the photolysis and control samples had similar decreases in average carbon

number over the four hours, which agrees with the shift toward lower molecular weights shown in these mass spectra in Figures 1 and 3.

Average O/C ratios reflect the extent of SOA oxidation, which is indirectly related to the volatility of the SOA compounds. Within the uncertainty for the calculated O/C ratios they do not change much with time, although subtle trends can be discerned. Previous studies of APIN SOA reactions in pure water have shown average O/C ratios to increase slowly with photolysis and decrease with hydrolysis,[66,67] and the same trends are observed here (Figure 4). In contrast, in presence of an aqueous oxidant, the average O/C ratio appears to increase for both the photolysis and control conditions. We observed a decrease in O/C ratios for HUM SOA photolysis and hydrolysis conditions in pure water (Figure 5), confirming results of our previous work.[24] The same trend was observed in the presence of H_2O_2. However, in presence $NaNO_3$ and NH_4NO_3, the average O/C ratio for the control conditions was approximately constant over time. These subtle differences in the behavior of aqueous SOA in the presence of aqueous oxidants versus in pure water shows that SOA aging in pure water does not fully represent the chemistry occurring in ambient cloud droplets.

Finally, the average N/C ratios were also calculated to check for the evidence of NH_4^+ or NO_3^- driven chemistry leading to stable organonitrogen compounds. As pointed out above, the peak abundances of NOC were small, typically below 2% of the highest peak and barely visible in Figures 1 and 3. We replotted Figures 1 and 3 on a logarithmic scale as Figures S11 and S12 to make it easier to see NOC peaks. NOC formed in the SOA + $NaNO_3$ systems under dark conditions likely formed through reactions of NO_3^- with epoxides in the SOA.[30] SOA aged with NH_4NO_3 under dark conditions produced a slightly higher N/C ratio than SOA aged with $NaNO_3$. N/C ratios in APIN SOA + NH_4NO_3 were found to be about 0.02, which agrees with the N/C ratio determined by Laskin et al. (2014) when they aged APIN ozonolysis SOA in the presence of gaseous ammonia.[68] N/C ratios for HUM SOA were found to be lower, with magnitudes of the order of 10^{-4}. The photolysis did not change the N/C ratio, however, it changed the mass distribution of NOC. The NOC peaks in the photolysis condition have higher relative abundances and appear at lower neutral masses than those in the control condition. It therefore seems

likely that the NOC peaks in the photolysis conditions are products of photo-induced decomposition of nitrogen-containing APIN SOA molecules.

CONCLUSION

Chemistry occurring in cloud and fog water is known to be an important aspect of SOA formation and aging. These atmospheric waters contain small concentrations of oxidants and inorganic salts, which may have various direct and indirect effects on aqueous reactions of SOA compounds. This study analyzed the effect of atmospheric oxidants (H_2O_2) and inorganic salts ($NaNO_3$ and NH_4NO_3) on the aging of aqueous SOA in the dark and under UV irradiation conditions. Our initial expectation was that the added solutes would not do much under dark conditions but would accelerate the photodegradation of dissolved SOA. However, we found that the presence of nitrate ions efficiently reduced dimer abundance in APIN SOA *without photolysis*, likely through catalysis of hydrolysis of dimeric esters. The unusual effect of nitrate ions will be particularly important in urban areas where large amounts of NO_x from cars lead to significant amounts of NO_3^- in the atmospheric waters (for example, in the Los Angeles area). These results show that it is important to consider the presence of inorganic salts in cloud or fog water when studying aqueous SOA aging, both in the dark and under irradiated conditions.

ASSOCIATED CONTENT

Supporting Information

The Supporting Information is available free of charge on the ACS Publications website at DOI:XXXX. It contains all of the mass spectra analyzed for this paper, a comparison of the spectral flux densities from the photolysis set-up and from the sun, the extraction efficiency of HUM SOA in water, and details on the OH steady-state concentration calculations.

AUTHOR INFORMATION

Corresponding Author

* E-mail: nizkorod@uci.edu

ORCID

Alexandra Klodt: 0000-0002-3558-972X

Julia Laskin: 0000-0002-4533-9644

Alexander Laskin: 0000-0002-7836-8417

Peng Lin: 0000-0002-3567-7017

Sergey A. Nizkorodov: 0000-0003-0891-0052

Dian Romonosky: 0000-0002-3940-1341

Notes

The authors declare no competing financial interest.

ACKNOWLEDGMENTS

The UCI team acknowledges support from the NSF grant AGS-1853639. DER thanks support from NSF through the graduate research fellowship program. The HRMS measurements were performed at the W.R. Wiley Environmental Molecular Sciences Laboratory (EMSL) – a national scientific user facility located at PNNL and sponsored by the Office of Biological and Environmental Research of the U.S. DOE.

REFERENCES

(1) Finlayson-Pitts, B. J.; Pitts, J. N. *Chemistry of the Upper and Lower Atmosphere : Theory, Experiments, and Applications*; Academic Press, 2000.

(2) Bouvier-Brown, N. C.; Goldstein, A. H.; Gilman, J. B.; Kuster, W. C.; De Gouw, J. A. In-Situ Ambient Quantification of Monoterpenes, Sesquiterpenes and Related Oxygenated Compounds during BEARPEX 2007: Implications for Gas- And Particle-Phase Chemistry. *Atmos. Chem. Phys.* **2009**, *9* (15), 5505–5518. https://doi.org/10.5194/acp-9-5505-2009.

(3) Kanakidou, M.; Seinfeld, J. H.; Pandis, S. N.; Barnes, I.; Dentener, F. J.; Facchini, M. C.; Van Dingenen, R.; Ervens, B.; Nenes, A.; Nielsen, C. J.; et al. Organic Aerosol and Global

Climate Modelling: A Review. *Atmos. Chem. Phys.* **2005**, *5* (4), 1053–1123. https://doi.org/10.5194/acp-5-1053-2005.

(4) Zhang, H.; Yee, L. D.; Lee, B. H.; Curtis, M. P.; Worton, D. R.; Isaacman-VanWertz, G.; Offenberg, J. H.; Lewandowski, M.; Kleindienst, T. E.; Beaver, M. R.; et al. Monoterpenes Are the Largest Source of Summertime Organic Aerosol in the Southeastern United States. *Proc. Natl. Acad. Sci. U. S. A.* **2018**, *115* (9), 2038–2043. https://doi.org/10.1073/pnas.1717513115.

(5) Kroll, J. H.; Seinfeld, J. H. Chemistry of Secondary Organic Aerosol: Formation and Evolution of Low-Volatility Organics in the Atmosphere. *Atmos. Environ.* **2008**, *42* (16), 3593–3624. https://doi.org/10.1016/J.ATMOSENV.2008.01.003.

(6) Atkinson, R. A.; Arey, J. Atmospheric Degradation of Volatile Organic Compounds. *Chem. Rev.* **2003**, *103* (12), 4305–4638. https://doi.org/10.1021/CR0206420.

(7) Calvert, J. G. (Jack G. *The Mechanisms of Atmospheric Oxidation of Aromatic Hydrocarbons*; Oxford University Press, 2002.

(8) Beck, M.; Winterhalter, R.; Herrmann, F.; Moortgat, G. K. The Gas-Phase Ozonolysis of α-Humulene. *Phys. Chem. Chem. Phys.* **2011**, *13* (23), 10970–11001. https://doi.org/10.1039/c0cp02379e.

(9) Hallquist, M.; Wenger, J. C.; Baltensperger, U.; Rudich, Y.; Simpson, D.; Claeys, M.; Dommen, J.; Donahue, N. M.; George, C.; Goldstein, A. H.; et al. The Formation, Properties and Impact of Secondary Organic Aerosol: Current and Emerging Issues. *Atmos. Chem. Phys* **2009**, *9*, 5155–5236.

(10) Herrmann, H.; Schaefer, T.; Tilgner, A.; Styler, S. A.; Weller, C.; Teich, M.; Otto, T. Tropospheric Aqueous-Phase Chemistry: Kinetics, Mechanisms, and Its Coupling to a Changing Gas Phase. *Chem. Rev.* **2015**, *115* (10), 4259–4334. https://doi.org/10.1021/cr500447k.

(11) McNeill, V. F. Aqueous Organic Chemistry in the Atmosphere: Sources and Chemical

Processing of Organic Aerosols. *Environ. Sci. Technol.* **2015**, *49* (3), 1237–1244. https://doi.org/10.1021/es5043707.

(12) Ng, N. L.; Canagaratna, M. R.; Zhang, Q.; Jimenez, J. L.; Tian, J.; Ulbrich, I. M.; Kroll, J. H.; Docherty, K. S.; Chhabra, P. S.; Bahreini, R.; et al. Organic Aerosol Components Observed in Northern Hemispheric Datasets from Aerosol Mass Spectrometry. *Atmos. Chem. Phys.* **2010**, *10* (10), 4625–4641. https://doi.org/10.5194/acp-10-4625-2010.

(13) Ervens, B.; Volkamer, R. Glyoxal Processing by Aerosol Multiphase Chemistry: Towards a Kinetic Modeling Framework of Secondary Organic Aerosol Formation in Aqueous Particles. *Atmos. Chem. Phys.* **2010**, *10* (17), 8219–8244. https://doi.org/10.5194/acp-10-8219-2010.

(14) Collett, J. L.; Bator, A.; Sherman, D.; Moore, K. F.; Hoag, K. J.; Demoz, B. B.; Rao, X.; Reilly, J. E. The Chemical Composition of Fogs and Intercepted Clouds in the United States. *Atmos. Res.* **2002**, *64* (1–4), 29–40. https://doi.org/10.1016/S0169-8095(02)00077-7.

(15) Collett, J. L.; Herckes, P.; Youngster, S.; Lee, T. Processing of Atmospheric Organic Matter by California Radiation Fogs. *Atmos. Res.* **2008**, *87* (3–4), 232–241. https://doi.org/10.1016/j.atmosres.2007.11.005.

(16) Mack, J.; Bolton, J. R. Photochemistry of Nitrite and Nitrate in Aqueous Solution: A Review. *J. Photochem. Photobiol. A Chem.* **1999**, *128* (1–3), 1–13. https://doi.org/10.1016/S1010-6030(99)00155-0.

(17) Nozière, B.; Fache, F.; Maxut, A.; Fenet, B.; Baudouin, A.; Fine, L.; Ferronato, C. The Hydrolysis of Epoxides Catalyzed by Inorganic Ammonium Salts in Water: Kinetic Evidence for Hydrogen Bond Catalysis. *Phys. Chem. Chem. Phys.* **2018**, *20* (3), 1583–1590. https://doi.org/10.1039/C7CP06790A.

(18) Nozière, B.; Dziedzic, P.; Córdova, A. Inorganic Ammonium Salts and Carbonate Salts Are Efficient Catalysts for Aldol Condensation in Atmospheric Aerosols. *Phys. Chem. Chem. Phys.* **2010**, *12* (15), 3864–3872. https://doi.org/10.1039/b924443c.

(19) Zhou, W.; Mekic, M.; Liu, J.; Loisel, G.; Jin, B.; Vione, D.; Gligorovski, S. Ionic Strength Effects on the Photochemical Degradation of Acetosyringone in Atmospheric Deliquescent Aerosol Particles. *Atmos. Environ.* **2019**, *198*, 83–88. https://doi.org/10.1016/J.ATMOSENV.2018.10.047.

(20) Mekic, M.; Brigante, M.; Vione, D.; Gligorovski, S. Exploring the Ionic Strength Effects on the Photochemical Degradation of Pyruvic Acid in Atmospheric Deliquescent Aerosol Particles. *Atmos. Environ.* **2018**, *185*, 237–242. https://doi.org/10.1016/J.ATMOSENV.2018.05.016.

(21) Huang, D. D.; Zhang, Q.; Cheung, H. H. Y.; Yu, L.; Zhou, S.; Anastasio, C.; Smith, J. D.; Chan, C. K. Formation and Evolution of AqSOA from Aqueous-Phase Reactions of Phenolic Carbonyls: Comparison between Ammonium Sulfate and Ammonium Nitrate Solutions. *Environ. Sci. Technol.* **2018**, *52* (16), 9215–9224. https://doi.org/10.1021/acs.est.8b03441.

(22) Bateman, A. P.; Nizkorodov, S. A.; Laskin, J.; Laskin, A. Photolytic Processing of Secondary Organic Aerosols Dissolved in Cloud Droplets. *Phys. Chem. Chem. Phys.* **2011**, *13* (26), 12199–12212. https://doi.org/10.1039/c1cp20526a.

(23) Nguyen, T. B.; Laskin, A.; Laskin, J.; Nizkorodov, S. A. Direct Aqueous Photochemistry of Isoprene High-NOx Secondary Organic Aerosol. *Phys. Chem. Chem. Phys.* **2012**, *14* (27), 9702–9714. https://doi.org/10.1039/c2cp40944e.

(24) Romonosky, D. E.; Li, Y.; Shiraiwa, M.; Laskin, A.; Laskin, J.; Nizkorodov, S. A. Aqueous Photochemistry of Secondary Organic Aerosol of α-Pinene and α-Humulene Oxidized with Ozone, Hydroxyl Radical, and Nitrate Radical. *J. Phys. Chem. A* **2017**, *121* (6), 1298–1309. https://doi.org/10.1021/acs.jpca.6b10900.

(25) Ji, H.; Lee, J.; Aiona, P. K.; Laskin, A.; Laskin, J.; Nizkorodov, S. A. Effect of Solar Radiation on the Optical Properties and Molecular Composition of Laboratory Proxies of Atmospheric Brown Carbon. *Environ. Sci. Technol.* **2014**, *48* (17), 10217–10226. https://doi.org/10.1021/es502515r.

(26) Lignell, H.; Epstein, S. A.; Marvin, M. R.; Shemesh, D.; Gerber, B.; Nizkorodov, S. Experimental and Theoretical Study of Aqueous Cis-Pinonic Acid Photolysis. *J. Phys. Chem. A* **2013**, *117* (48), 12930–12945. https://doi.org/10.1021/jp4093018.

(27) Shaffer, G. W.; Doerr, A. B.; Purzycki, K. L. Photoisomerization of Nopinone. *Org. Chem* **1972**, *37* (1), 25–29.

(28) Aljawhary, D.; Zhao, R.; Lee, A. K. Y.; Wang, C.; Abbatt, J. P. D. Kinetics, Mechanism, and Secondary Organic Aerosol Yield of Aqueous Phase Photo-Oxidation of α-Pinene Oxidation Products. *J. Phys. Chem. A* **2016**, *120* (9), 1395–1407. https://doi.org/10.1021/acs.jpca.5b06237.

(29) Hu, K. S.; Darer, A. I.; Elrod, M. J. Thermodynamics and Kinetics of the Hydrolysis of Atmospherically Relevant Organonitrates and Organosulfates. *Atmos. Chem. Phys.* **2011**, *11* (16), 8307–8320. https://doi.org/10.5194/acp-11-8307-2011.

(30) Darer, A. I.; Cole-Filipiak, N. C.; O'Connor, A. E.; Elrod, M. J. Formation and Stability of Atmospherically Relevant Isoprene-Derived Organosulfates and Organonitrates. *Environ. Sci. Technol.* **2011**, *45* (5), 1895–1902. https://doi.org/10.1021/es103797z.

(31) Häkkinen, S. A. K.; McNeill, V. F.; Riipinen, I. Effect of Inorganic Salts on the Volatility of Organic Acids. *Environ. Sci. Technol.* **2014**, *48* (23), 13718–13726. https://doi.org/10.1021/es5033103.

(32) Wang, B.; O'Brien, R. E.; Kelly, S. T.; Shilling, J. E.; Moffet, R. C.; Gilles, M. K.; Laskin, A. Reactivity of Liquid and Semisolid Secondary Organic Carbon with Chloride and Nitrate in Atmospheric Aerosols. *J. Phys. Chem. A* **2015**, *119*, 4498–4508. https://doi.org/10.1021/jp510336q.

(33) Ziemann, P. J.; Atkinson, R. Kinetics, Products, and Mechanisms of Secondary Organic Aerosol Formation. *Chem. Soc. Rev.* **2012**, *41* (19), 6582–6605. https://doi.org/10.1039/c2cs35122f.

(34) Tilgner, A.; Bräuer, P.; Wolke, R.; Herrmann, H. Modelling Multiphase Chemistry in

Deliquescent Aerosols and Clouds Using CAPRAM3.0i. *J. Atmos. Chem.* **2013**, *70* (3), 221–256. https://doi.org/10.1007/s10874-013-9267-4.

(35) Deguillaume, L.; Leriche, M.; Desboeufs, K.; Mailhot, G.; George, C.; Chaumerliac, N. Transition Metals in Atmospheric Liquid Phases: Sources, Reactivity, and Sensitive Parameters. *Chem. Rev.* **2005**, *105* (9), 3388–3431. https://doi.org/10.1021/CR040649C.

(36) Romonosky, D. E.; Laskin, A.; Laskin, J.; Nizkorodov, S. A. High-Resolution Mass Spectrometry and Molecular Characterization of Aqueous Photochemistry Products of Common Types of Secondary Organic Aerosols. *J. Phys. Chem. A* **2015**, *119* (11), 2594–2606. https://doi.org/10.1021/jp509476r.

(37) Nguyen, T. B.; Bateman, A. P.; Bones, D. L.; Nizkorodov, S. A.; Laskin, J.; Laskin, A. High-Resolution Mass Spectrometry Analysis of Secondary Organic Aerosol Generated by Ozonolysis of Isoprene. *Atmos. Environ.* **2010**, *44* (8), 1032–1042. https://doi.org/10.1016/J.ATMOSENV.2009.12.019.

(38) Updyke, K. M.; Nguyen, T. B.; Nizkorodov, S. A. Formation of Brown Carbon via Reactions of Ammonia with Secondary Organic Aerosols from Biogenic and Anthropogenic Precursors. *Atmos. Environ.* **2012**, *63*, 22–31. https://doi.org/10.1016/J.ATMOSENV.2012.09.012.

(39) Madronich, S. ACOM: Quick TUV http://cprm.acom.ucar.edu/Models/TUV/Interactive_TUV/ (accessed Jul 11, 2019).

(40) Bateman, A. P.; Laskin, J.; Laskin, A.; Nizkorodov, S. A. Applications of High-Resolution Electrospray Ionization Mass Spectrometry to Measurements of Average Oxygen to Carbon Ratios in Secondary Organic Aerosols. *Environ. Sci. Technol.* **2012**, *46* (15), 8315–8324. https://doi.org/10.1021/es3017254.

(41) Bateman, A. P.; Nizkorodov, S. A.; Laskin, J.; Laskin, A. Time-Resolved Molecular Characterization of Limonene/Ozone Aerosol Using High-Resolution Electrospray Ionization Mass Spectrometry. *Phys. Chem. Chem. Phys.* **2009**, *11* (36), 7931–7942.

https://doi.org/10.1039/b905288g.

(42) Nguyen, T. B.; Roach, P. J.; Laskin, J.; Laskin, A.; Nizkorodov, S. A. Atmospheric Chemistry and Physics Effect of Humidity on the Composition of Isoprene Photooxidation Secondary Organic Aerosol. *Atmos. Chem. Phys* **2011**, *11*, 6931–6944. https://doi.org/10.5194/acp-11-6931-2011.

(43) Nguyen, T. B.; Laskin, J.; Laskin, A.; Nizkorodov, S. A. Nitrogen-Containing Organic Compounds and Oligomers in Secondary Organic Aerosol Formed by Photooxidation of Isoprene. *Environ. Sci. Technol.* **2011**, *45* (16), 6908–6918. https://doi.org/10.1021/es201611n.

(44) Nizkorodov, S. A.; Laskin, J.; Laskin, A. Molecular Chemistry of Organic Aerosols through the Application of High Resolution Mass Spectrometry. *Phys. Chem. Chem. Phys.* **2011**, *13* (9), 3612–3629. https://doi.org/10.1039/c0cp02032j.

(45) Willoughby, R.; Sheehan, E.; Mitrovich, S. A Global View of LC/MS. In *A Global View of LC/MS*; Global View Publishing: Pittsburg, PA, 1998; pp 311–315.

(46) Leenheer, J. A.; Rostad, C. E.; Gates, P. M.; Furlong, E. T.; Ferrer, I. Molecular Resolution and Fragmentation of Fulvic Acid by Electrospray Ionization/Multistage Tandem Mass Spectrometry. *Anal. Chem.* **2001**, *73* (7), 1461–1471. https://doi.org/10.1021/ac0012593.

(47) Kind, T.; Fiehn, O. Seven Golden Rules for Heuristic Filtering of Molecular Formulas Obtained by Accurate Mass Spectrometry. *BMC Bioinformatics* **2007**, *8*, 105. https://doi.org/10.1186/1471-2105-8-105.

(48) Bones, D. L.; Henricksen, D. K.; Mang, S. A.; Gonsior, M.; Bateman, A. P.; Nguyen, T. B.; Cooper, W. J.; Nizkorodov, S. A. Appearance of Strong Absorbers and Fluorophores in Limonene-O3 Secondary Organic Aerosol Due to NH4+-Mediated Chemical Aging over Long Time Scales. *J. Geophys. Res. Atmos.* **2010**, *115* (5), D05203. https://doi.org/10.1029/2009JD012864.

(49) Laskin, A.; Laskin, J.; Nizkorodov, S. A. Chemistry of Atmospheric Brown Carbon. *Chemical*

Reviews. American Chemical Society 2015, pp 4335–4382. https://doi.org/10.1021/cr5006167.

(50) Baltensperger, U.; Kalberer, M.; Dommen, J.; Paulsen, D.; Alfarra, M. R.; Coe, H.; Fisseha, R.; Gascho, A.; Gysel, M.; Nyeki, S.; et al. Secondary Organic Aerosols from Anthropogenic and Biogenic Precursors. *Faraday Discuss.* **2005**, *130*, 265–278. https://doi.org/10.1039/b417367h.

(51) Reinhardt, A.; Emmenegger, C.; Gerrits, B.; Panse, C.; Dommen, J.; Baltensperger, U.; Zenobi, R.; Kalberer, M. Ultrahigh Mass Resolution and Accurate Mass Measurements as a Tool To Characterize Oligomers in Secondary Organic Aerosols. *Anal. Chem.* **2007**, *79* (11), 4074–4082. https://doi.org/10.1021/AC062425V.

(52) Tolocka, M. P.; Jang, M.; Ginter, J. M.; Cox, F. J.; Kamens, R. M.; Johnston, M. V. Formation of Oligomers in Secondary Organic Aerosol. *Environ. Sci. Technol.* **2004**, *38* (5), 1428–1434. https://doi.org/10.1021/es035030r.

(53) Gao, Y.; Hall, W. A.; Johnston, M. V. Molecular Composition of Monoterpene Secondary Organic Aerosol at Low Mass Loading. *Environ. Sci. Technol.* **2010**, *44* (20), 7897–7902. https://doi.org/10.1021/es101861k.

(54) Kristensen, K.; Watne, Å. K.; Hammes, J.; Lutz, A.; Petäjä, T.; Hallquist, M.; Bilde, M.; Glasius, M. High-Molecular Weight Dimer Esters Are Major Products in Aerosols from α-Pinene Ozonolysis and the Boreal Forest. *Environ. Sci. Technol. Lett.* **2016**, *3* (8), 280–285. https://doi.org/10.1021/acs.estlett.6b00152.

(55) Glasius, M.; Duane, M.; Larsen, B. R. Determination of Polar Terpene Oxidation Products in Aerosols by Liquid Chromatography–ion Trap Mass Spectrometry. *J. Chromatogr. A* **1999**, *833* (2), 121–135. https://doi.org/10.1016/S0021-9673(98)01042-5.

(56) Kahnt, A.; Iinuma, Y.; Mutzel, A.; Böge, O.; Claeys, M.; Herrmann, H. Campholenic Aldehyde Ozonolysis: A Mechanism Leading to Specific Biogenic Secondary Organic Aerosol Constituents. *Atmos. Chem. Phys.* **2014**, *14* (2), 719–736.

https://doi.org/10.5194/acp-14-719-2014.

(57) Venkatachari, P.; Hopke, P. K. Characterization of Products Formed in the Reaction of Ozone with α-Pinene: Case for Organic Peroxides. *J. Environ. Monit.* **2008**, *10* (8), 966–974. https://doi.org/10.1039/b804357d.

(58) Camredon, M.; Hamilton, J. F.; Alam, M. S.; Wyche, K. P.; Carr, T.; White, I. R.; Monks, P. S.; Rickard, A. R.; Bloss, W. J. Distribution of Gaseous and Particulate Organic Composition during Dark Alpha-Pinene Ozonolysis. *Atmos. Chem. Phys.* **2010**, *10* (6), 2893–2917. https://doi.org/10.5194/acp-10-2893-2010.

(59) Witkowski, B.; Gierczak, T. Early Stage Composition of SOA Produced by α-Pinene/Ozone Reaction: α-Acyloxyhydroperoxy Aldehydes and Acidic Dimers. *Atmos. Environ.* **2014**, *95*, 59–70. https://doi.org/10.1016/j.atmosenv.2014.06.018.

(60) Kahnt, A.; Vermeylen, R.; Iinuma, Y.; Safi Shalamzari, M.; Maenhaut, W.; Claeys, M. High-Molecular-Weight Esters in α-Pinene Ozonolysis Secondary Organic Aerosol: Structural Characterization and Mechanistic Proposal for Their Formation from Highly Oxygenated Molecules. *Atmos. Chem. Phys.* **2018**, *18* (11), 8453–8467. https://doi.org/10.5194/acp-18-8453-2018.

(61) Mang, S. A.; Henricksen, D. K.; Bateman, A. P.; Andersen, M. P. S.; Blake, D. R.; Nizkorodov, S. A. Contribution of Carbonyl Photochemistry to Aging of Atmospheric Secondary Organic Aerosol. *J. Phys. Chemsitry A* **2008**, No. 112, 8337–8344. https://doi.org/10.1021/jp804376c.

(62) Epstein, S. A.; Blair, S. L.; Nizkorodov, S. A. Direct Photolysis of α-Pinene Ozonolysis Secondary Organic Aerosol: Effect on Particle Mass and Peroxide Content. *Environ. Sci. Technol.* **2014**, *48*, 11251–11258. https://doi.org/10.1021/es502350u.

(63) Bender, M. L. Mechanisms of Catalysis of Nucleophilic Reactions of Carboxylic Acid Derivatives. *Chem. Rev.* **1960**, *60* (1), 54–107.

(64) King, R.; Bonfiglio, R.; Fernandez-Metzler, C.; Miller-Stein, C.; Olah, T. Mechanistic

Investigation of Ionization Suppression in Electrospray Ionization. *J. Am. Soc. Mass Spectrom.* **2000**, *11* (11), 942–950. https://doi.org/10.1016/S1044-0305(00)00163-X.

(65) Ng, N. L.; Kroll, J. H.; Keywood, M. D.; Bahreini, R.; Varutbangkul, V.; Flagan, R. C.; Seinfeld, J. H.; Lee, A.; Goldstein, A. H. Contribution of First- versus Second-Generation Products to Secondary Organic Aerosols Formed in the Oxidation of Biogenic Hydrocarbons. *Environ. Sci. Technol.* **2006**, *40* (7), 2283–2297. https://doi.org/10.1021/es052269u.

(66) Thomas Brinkmann; Philip Hörsch; Daniel Sartorius, A.; Frimmel, F. H. Photoformation of Low-Molecular-Weight Organic Acids from Brown Water Dissolved Organic Matter. *Environ. Sci. Technol.* **2003**, *37* (18), 4190–4198. https://doi.org/10.1021/ES0263339.

(67) Kujawinski, E. B.; Del Vecchio, R.; Blough, N. V.; Klein, G. C.; Marshall, A. G. Probing Molecular-Level Transformations of Dissolved Organic Matter: Insights on Photochemical Degradation and Protozoan Modification of DOM from Electrospray Ionization Fourier Transform Ion Cyclotron Resonance Mass Spectrometry. *Mar. Chem.* **2004**, *92* (1–4 SPEC. ISS.), 23–37. https://doi.org/10.1016/j.marchem.2004.06.038.

(68) Laskin, J.; Laskin, A.; Nizkorodov, S. A.; Roach, P.; Eckert, P.; Gilles, M. K.; Wang, B.; Ji, H.; Lee, J.; Hu, Q. Molecular Selectivity of Brown Carbon Chromophores. *Environ. Sci. Technol.* **2014**, *48* (20), 12047–12055. https://doi.org/10.1021/es503432r.

TOC image

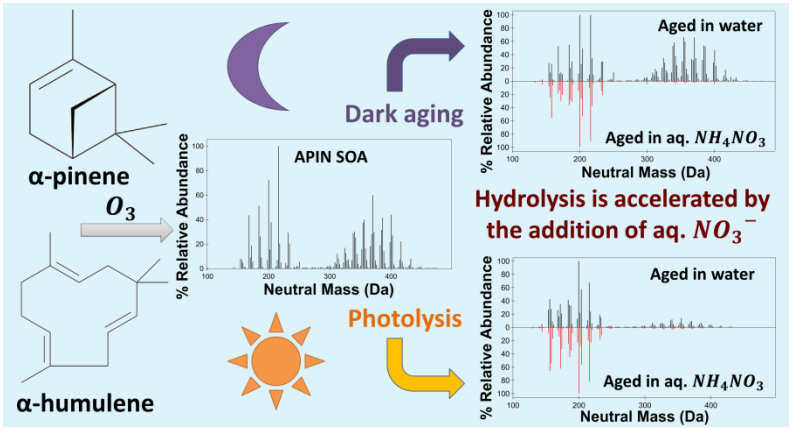
α-pinene
O_3
α-humulene
APIN SOA
% Relative Abundance
Neutral Mass (Da)
Dark aging
Photolysis
Aged in water
Aged in aq. NH_4NO_3
Hydrolysis is accelerated by the addition of aq. NO_3^-